

# Paper I



## An anatomy of interactions among species in a seasonal world

Gunnar Sandvik, Knut L. Seip and Harald Pleym

Sandvik, G., Seip, K. L. and Pleym, H. 2002. An anatomy of interactions among species in a seasonal world. – *Oikos* 99: 260–271.

Mathematical models merging biological and predictable seasonal dynamics were used to simulate four types of organism interactions: competition, prey-predation, mutualism and facilitation. By analysing trajectories for biomass in phase portraits (i.e. species 1 biomass plotted against species 2 biomass) graphically and numerically, we found that each of the four interaction types showed characteristic patterns (“fingerprints”) in phase space. All the four interaction types could be distinguished, even though their time trajectories were strongly modified by seasonal forces. For each of the interaction types, we were able to identify characteristics of the interaction that most strongly distinguished it from the others. We could also assess the relative effect of species characteristics and seasonality on each of the four interactions. The simulations indicate that prey-predation is strongly influenced by seasonal forces and by the characteristics of the predator and its prey. A system variability index got a high value (SVI) = 0.167 relative to those of the other interaction types (competition 0.01, mutualism 0.007 and facilitation 0.005). The result was obtained by calculating angles between successive vectors linking pairs of samples and the positive x-axis and arranging these as frequency histograms for each of the four quadrants of the phase portrait. In an effort to capture circular motions and other characteristics of the trajectories sampled, angle frequencies were analysed using multivariate statistics (PCA), yielding “characteristic directions” in phase space. We believe that the characteristic patterns identified also will be found in real time series.

*G. Sandvik and H. Pleym, Høgskolen i Telemark, NO-3914 Porsgrunn, Norway (gumsa2@frisurf.no). – K. L. Seip, Høgskolen i Oslo, Cort Adlersgt 30, NO-0254 Oslo, Norway.*

Ecosystems at temperate latitudes are seasonally driven. Forced by changes in light and temperature, cyclic growth commences in spring and declines in autumn. Seasonality is caused by many abiotic factors changing in concert. At smaller scales, stochastic fluctuations in atmospheric conditions (especially with respect to precipitation, wind velocity and direction, and cloud cover) are superimposed upon essentially predictable seasonal cycles. This paper focuses on the relative effect of seasonality on reciprocal two-species interactions.

We restrict the approach to the four fundamental ecological interactions, competition, prey-predation, mutualism and facilitation. Our objective is to examine effects of seasonality on these interactions by examining synoptic biomass time series. We hypothesize that dif-

ferent types of species interactions leave patterns in their phase-space trajectories that separate them from other interactions, and that seasonality will have different effects on the four types of interactions. If the hypotheses are valid, we may also enhance our ability to predict the fate of interacting species during unidirectional environmental changes (e.g. oligotrophication or climatic change).

Although several theories predict the conditions under which a particular species interaction should be strong, the actual strength has proved difficult to determine quantitatively (Sarnelle 1994, Thompson 1999). From the literature we have identified three methods: i) studies of time series by cross correlation and other time lag detection techniques (McCaughey and Murdoch

---

Accepted 22 April 2002

Copyright © OIKOS 2002  
ISSN 0030-1299

1987, Matveev, 1995), ii) regressions between biomass measures of species with different ecological roles (McQueen et al. 1986, Mazumder and Havens 1998), iii) studies of phase portraits (Gilpin 1973, Seip 1997). This work is based on the last approach.

We simulate the fate of two species systems of the four interaction types in non-seasonal and seasonal environments. Simulated time trajectories are analysed using a method we have named the angle frequency method (AFM). Since we define the characteristics of each species and their interactions through our choice of equations and parameter values, we can assess the success of the method. If the method is successful for a simulated system, we may at least hypothesize that it will also work with data observed in situ.

A partial contribution for the ability of species to increase in biomass under favourable ambient conditions is often formulated in terms of response functions for their growth and mortality to abiotic factors. Seip and Reynolds (1995) showed that many phytoplankton species are abundant under in situ conditions that correspond to optimal growth under laboratory conditions. For example, species that have a high affinity for phosphorus (P) are abundant under P shortage (Seip and Reynolds 1995). It also appears that species has a combination, or bundle, of favourable physiological characteristics that reflect the particular abiotic regime in which they are actually found. In the present study, we formulate this as one single response to a generalized seasonal forcing function, the species' "niche". The form is a bell-shaped curve. The peaks of two bell curves are shifted relative to each other along the time axis if two species differ in their niches. Changes in biomass can also occur via immigration or emigration processes, but these demographic factors are considered constant and thus not included in the model.

Although the present study is a modelling exercise, the parameters for algal characteristics and for seasonality effects are primarily based on data from observations taken from the central monitoring station Skreia, Lake Mjøsa, Norway. Mixed samples (phytoplankton and chemical parameters) were taken from the upper 10 m at regular intervals of approximately 14 days over the algal growth season (Kjellberg 1986–1998).

## Materials and methods

The method sections consist of three parts. First we characterize, and mathematically describe, the four types of species interactions that we would find in a real lake system. Secondly we give the basic model formulations and address parameterization; finally we describe the AFM, for identifying species interactions from biomass trajectories.

## Species interactions

### Prey-predation

This interaction describes the situation when one species is the food of another. Food shortage for the predator species is as important as predation for the prey species. The predator response tracks that of the prey, but the prey and predator responses are not exactly reciprocal, as shown by Reynolds et al. (1982). Matveev (1995) for example observed that the biomass of a predator was a delayed function of prey biomass (8 days) and prey biomass was a delayed function of predator biomass (13 days). McCauley and Murdoch (1987) found that a *Daphnia* (predator) cycle lagged behind the algal cycle (prey) by 0.33 of the period of the algal cycle, confirming the asymmetry in lag times. They also found a significant positive relationship between the average period of *Daphnia* and algal cycles (range for both species 25–53 days;  $r = 0.65$ ,  $p < 0.01$ ). However, lag time depends upon predation intensity and prey recruitment intensity as pointed out by Matveev (1995). Grazing by zooplankton in many lake ecosystems clearly follows after the growth of the first spring bloom of phytoplankton (Sommer et al. 1986). Prey-predation is hypothesized to be most important at low levels of physical stress (Bertness and Callaway 1994), and is here described by equations adopted from Kretzschmar et al. (1993):

$$dP/dt = P[r((1 - P/K) - gZ/(1 + hP)) - d_p] \quad (1)$$

$$dZ/dt = ZgeP/(1 + hP) - d_z \quad (2)$$

where P, r, K and  $d_p$  are biomass, maximal growth rate, carrying capacity and death rate respectively of the phytoplankton prey species. Z is biomass and  $d_z$  is death rate of the zooplankton species, g is attack rate (ingestion rate, range 0.0–1.0) of zooplankton on phytoplankton, h is product of attack rate and handling time for the zooplankton, and e is conversion efficiency of prey biomass into predator biomass (range 0.0–1.0). A Holling type II functional response (Yodzis 1989) describes the zooplankton ingestion rate, where the maximum rate is  $g/h$  and the half saturation constant is  $1/h$ .

### Competition

When two species jointly utilize a resource in short supply, we have competition. The differential equations (3, for competitor 1) and (4, for competitor 2) capture essential features of competition. We assume here that a nutrient resource is in short supply during the interval of competition. Competition is assumed to be strong during intermediate levels of physical stress and intermediate levels of prey-predation (Bertness and Callaway 1994). Equations to describe competition are chosen similar to those used by Kretzschmar et al. (1993):

$$dP_1/dt = P_1[r_1(1 - P_1/K_1 - a_{12}P_2/K_1) - d_1] \quad (3)$$

$$dP_2/dt = P_2[r_2(1 - P_2/K_2 - a_{21}P_1/K_2) - d_2] \quad (4)$$

where  $P_i$ ,  $K_i$ ,  $r_i$ , and  $d_i$  are biomass, carrying capacity, growth rate and death rates respectively of phytoplankton species  $i$ ,  $a_{12}$  and  $a_{21}$  are competition coefficients. In principle, equations for competition should include both equations for the competing species and for the resources for which they compete, like in many aquatic ecosystem models (Seip et al. 1991a). However, such complete forms can, under certain conditions, be shown to reduce to Lotka-Volterra type equations (Yodzis 1989). In these equations the resources are implicitly included through the parameters: growth rate,  $r = f(a_{ij}, L)$ , carrying capacity,  $K = g(a_{ij}, L)$ , the competition coefficients,  $a_{ij} = h(a_{ik}, a_{jk}, L_k)$ , where  $a_{ij}$  is the probability per unit time that the consumer species  $i$  capture and consume an item of the resource,  $j$  and  $L_k$ , the carrying capacity of resource  $k$  (Yodzis 1989).

In a phase diagram with competitor 1 on the x-axis and competitor 2 on the y-axis, we would predict that as the biomass of one competitor increases, the biomass of the other competitor decreases.

#### Mutualism

Positive interactions can broadly be defined as all non-destructive interactions among two or more species that positively affect at least one of the species involved. In this study, we focus on the direct, non-trophic positive interaction. Positive interactions have been suggested to be common in physically harsh conditions, and during high grazing pressure (Bertness and Callaway 1994). Chesson and Huntly (1997), on the other hand, claim that harshness favours coexistence only when it creates spatial or temporal niche opportunities. Mutualism also describes the situation where one partner participates as a forager, like bees and other as pollinators. A model for mutualism was developed by Wright (1989) and is used here. Its characteristic feature is that the benefits from mutualism saturate, or that factors outside mutualism act to create positively sloped isoclines (saturation) in phase diagrams:

$$dP_1/dt = P_1[r_1((1 - P_1/K_1) + pP_2/(1 + hP_2)) - d_1] \quad (5)$$

$$dP_2/dt = P_2[r_2((1 - P_2/K_2) + pP_1/(1 + hP_1)) - d_2] \quad (6)$$

where  $p$ , the mutuality rate (range 0.0–1.0) is a parameter describing the strength of the mutualistic effect. Both mutualists incorporate a type II functional response where  $h$  (handling time) is a constraint on one species' ability to physically utilize the benefit of its mutualistic partner. A classic example is the time consumed by a bee collecting pollen (Lindsley 1958). The other parameters are as defined above. The equations for the two species,  $P_1$  and  $P_2$ , both have the same form

as the form for prey species in the equations for prey-predation. This is now the logistic equation with a term added to include the per capita benefits of interacting with the population of a mutualistic partner. Increasing  $p$  and lowering  $h$  increase the benefits of mutualism. Facultative mutualism (i.e. one or both beneficiaries continue to grow when their benefactor declines) is described by positive growth rates. This implies that two facultative mutualistic organisms would always reach a stable non-negative equilibrium for biologically meaningful parameter values (Wright 1989). Wright suggests that obligate mutualism can be described with the same equations, but with negative  $r$  values, that is, if  $P_2$  declines, the biomass of species  $P_1$  declines and vice versa. A doubly obligate mutualism either has no positive equilibrium, or two equilibria, one stable and one unstable. The latter requires threshold population densities for the species to avoid extinction at low populations and infinite growth at high populations (Wright 1989).

#### Facilitation or engineering species

Facilitation would mean that one species ( $F$ ) facilitates the presence of another ( $G$ ) that gains an advantage from the first, whereas the latter may drive down the biomass of the first by competing with it. The engineering concept developed by Gurney and Lawton (1996) and Jones et al. (1997) is slightly different from the present concept of facilitation, as the gainer does not necessarily have negative effect on the engineer. Facilitation can be observed in many sequences of succession when a species conditions the environment for another. A hypothetical situation might be N-fixing algae increasing aquatic nitrogen concentrations and thereby allowing phytoplankton with higher nitrogen requirements to outcompete the benefactor. To model this situation, we use a competition formulation for the facilitator (7) and a mutuality formulation for the gainer (8):

$$dF/dt = F[r_f(1 - F/K_f - aG/K_f) - d_f] \quad (7)$$

$$dG/dt = G[r_g((1 - G/K_g) + pF/(1 + hF)) - d_g] \quad (8)$$

All parameters are defined and explained under competition (facilitator) and mutualism (gainer) above.

#### The model and data parameterization

The equations (1–8) are solved numerically (Fehlberg fourth–fifth order Runge-Kutta method) using the computer package Maple (Waterloo Maple, 1998. Maple V, Release 5, Waterloo Maple, Inc.).

Seasonal forcing is imposed on the growth rate  $r_i$  in eq. (1) and (3–8) in the form of a Gaussian function (eq. 9) representing the abiotic factors (i.e. light, nutri-

ents, temperature, etc.) cyclic alterations between enhancing and inhibiting growth. In the case of a predator, (eq. 2), no seasonal forcing is imposed as the predator always tracks the prey. Seasonal forces permit species to obtain different niches. The match of their physical requirements (i.e. temperature optimum, nutrient affinity, etc.), with the ever-changing physical conditions produced by seasonality; result in competitive advantages and disadvantages (Chesson and Huntly 1997).

As our prime aim is the comparison of how seasonality affects different interactions, we include seasonality in both the intraspecific and the interspecific terms of eq. (1) and (3–8). To increase realism, both interacting species (except predator in the prey-predation interaction) are externally forced by truncated and repeated Gaussian functions. Niche difference (i.e. number of days between the two interacting species' growth optima) is described by a relative shift in the midpoints of the two Gaussian functions:

$$r_i = \exp[-((t + N_s)/\sigma_s)^2] \quad (9)$$

The intrinsic growth rate,  $r_i$ , shows growth under optimal conditions.  $N_s$ ,  $\sigma_s$  and  $t$ , symbolize niche difference, width of the Gaussian function (1 year) and time respectively. The width of each Gaussian distribution is calculated as  $\sigma_s = \sqrt{2 \times \text{base} \times \text{frac}}$ , where  $\text{base} = 2(\pi/\omega)$ ,  $\text{frac} = 0.2$  and  $\omega = 0.25$ . Thus, within an annual period of 25 time steps, both the width of the Gaussian bell shape and the shift between the two bell

shapes are adjustable, facilitating the simulation of various seasonal forces (more details in Seip 1997 and Seip and Pleym 2000).

Deterministic equilibrium is a "fuzzy" value around which the biological system fluctuates (Renshaw 1991). However we use a set of standard parameter values, which approximate dynamic coexistence, serving as a state of reference for all simulations of the four interactions.

The carrying capacity term,  $K_i$ , summarizes intraspecific density dependence and produce a decrease in the growth rate as a function of the weighted biomass,  $P$ , of the  $j$  phytoplankton species present. The  $a_{ij}$  values give weights to interspecific density dependence. Published parameter ranges and our choice of standard parameter values, selected on the basis of data from lake Mjøsa, are shown in Table 1. We use parameters typical for functional species groups rather than for single species in accordance with the usual method for modelling aquatic systems.

### The angle frequency method (AFM)

The AFM method has been examined in two earlier studies. Seip (1997) developed a somewhat similar method, "the key factor" method, to characterize interaction. Seip and Pleym (2000) developed a first version of the AFM and applied it to the study of competition and prey-predation for simulated two-species systems that was exposed to increasingly seasonal environments.

Table 1. Published parameter ranges for primary producers (phytoplankton) and consumer (zooplankton) including our choice of standard values for prey (all interactions) and consumer (prey-predation only). Some parameter values are selected outside published ranges to produce typical model outputs.

Parameter (unit)	Published ranges		Standard parameter settings				
	Producer	Consumer	Competitor	Predator	Mutualist	Facilitator	Gainer
Maximum growth rates, $r_i$ <sup>(1)</sup> , (day <sup>-1</sup> )	0.23–3.40	0.12–0.82	1.7		1.7	1.7	1.7
Carrying capacity, $K_i$ , (µg c l <sup>-1</sup> )	20–50 <sup>(2)</sup>	20–50 <sup>(3)</sup>	400			400	400
Competition coefficients, $\alpha_{ij}$ , (1)	0.5–1.5 <sup>(4)</sup>		0.5			0.1	
Ingestion rate, $\gamma$ , (day × µg l <sup>-1</sup> ) <sup>-1</sup>		0.08–0.3 <sup>(7)</sup>		0.09			
Handling time, $h$ , (1)				0.0006			0.9
Mutuality rate, $\pi$ , (1)					0.8 <sup>(9)</sup>		0.08
Conversion efficiency, $\epsilon$ , (1)	1	0.2–0.5		0.08			
Niche difference, $N_s$ , (days)			14		14	14	14
Mortality rate, (day <sup>-1</sup> )			0.15	0.35	0.15	0.15	0.15
Initial population, (µg c l <sup>-1</sup> )			10	10	10	10	10

(1) Andersen (1997:272).

(2) About ±95% CI for summer average biomass at TP = 20 mg m<sup>-3</sup> (assuming only TP-limited growth, Seip et al. 1992: 60, 66 and Chl-a:C ratio of 1:50).

(3) At 20 mgP m<sup>-3</sup> zooplankton and phytoplankton are about equal in magnitude, Andersen (1997: 161).

(4) Kretzchmar et al. (1993) use  $\alpha_{12} = \alpha_{21} = 0.5$  (if  $K_1 = K_2$ ).

(5) Range for "idealized" phytoplankton spp. quoted by Andersen (1997: 48).

(6) Calculated as mean value of threshold food level for positive net growth and incipient level (saturated ingestion) from Andersen (1997:79, and Table A11.8), P:C ratio in phytoplankton is about 1:50.

(7) Andersen (1997: 78) and Seip et al. (1991a, b).

(8) For gainers, this parameter is set to 0.3 as a standard. This gives a moderate positive growth response for the gainer.

(9) For mutualists, this parameter is set to 0.8 as a standard. This give a moderate positive mutualistic effect due to a relatively low negative contribution from interspecific effects.

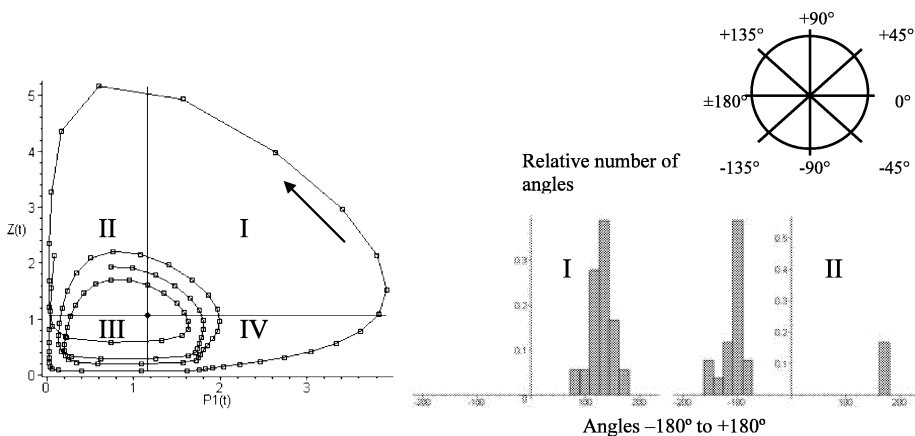


Fig. 1. Example phase portrait (prey-predation) demonstrating trajectory and two resulting angle histograms (angles with the positive x-axis) for the quadrants I and II. The arrow has an angle of approximately  $+135^\circ$  with the x-axis.

In this study, the simulated time trajectories are sampled, as we would have done in a real lake ecosystem. Then we construct phase plots,  $x$ ,  $y$ , with species 1 (prey) along the  $x$ -axis and species 2 (predator) along the  $y$ -axis. Since competition normally implies that one species decreases in biomass when another species increases in biomass, an “ideal” competition in a non-seasonal environment would appear as a line between the upper left corner to the lower right corner in phase space and show an angle  $\nu = 135^\circ$  with the positive  $x$ -axis. “Ideal” mutualism between equal partners would produce a line of  $\nu = 45^\circ$  through the origin. Prey-predation will show a counterclockwise rotation when the prey is depicted on the  $x$ -axis and the predator on the  $y$ -axis.

We construct angle-histograms as “fingerprints” for all the interactions. The histograms show the angles,  $\nu$ , between an interaction’s trajectory in phase space (the line between pairs of “samples”) and the positive  $x$ -axis. If trajectories rotate counterclockwise, the angles are defined as positive. We divide the angles into segments of  $18^\circ$ , giving a total of 21 bars in the histogram for one quadrant (Fig. 1).

We assess the AFM capacity of detecting the various interactions under seasonal conditions by running PCA analysis on trajectories from eight parameter combinations for all types of ecological interactions (i.e. 32 simulations, all parameter combinations (2–8) as compared to standard (1)):

1. All parameters at their standard values (Table 1)
- 2–3. Prey-predation: predator ingestion rate reduced by 10% and 20%,

Competition, mutualism and facilitation: niche difference increased by 10% and 20%

- 4–5.  $K$  of prey/late starter increased by 10% and 20%,
- 6–8.  $r$  of prey/late starter increased by 5%, 10% and 15%.

The PCA analyses are carried out with cross validation and normalized data (data divided by 1 standard deviation and thus expressed in different units than the biomass units).

We measure the sensitivity of the different interactions to changes in the parameter values by calculating a system variability index (SVI), as the area of swarms of points representing each interaction in the PCA score plot. We normalize each area by multiplying by  $1/\text{total area}$  of the score plot. We also compare the variance within classes of angles from the eight manipulations of the parameters for the four interactions. These variances are averaged over the 84 classes of angles to give a representative measure for each interaction.

## Results

Several simulations are performed in order to investigate the effect of introducing seasonality and niche difference to the four types of species interaction. Figure 2–5 below show selected results that depict essential features of the ecological interactions. When a biological two-species system at (dynamic) equilibrium is exposed to seasonal forces we regard it as unaffected if the relative distribution of the two species biomasses

remains unchanged (i.e. the two biomass time series tracks the seasonal changes in concert). Our simulations show that when seasonality interferes with the biological dynamics, other patterns may result.

Figure 2a shows an oscillating prey-predator interaction with a fast growing, but modestly edible ( $e = 0.08$ , range 0.0–1.0) phytoplankton grazed by a zooplankton with a low ingestion rate ( $g = 0.09$ , range 0.0–1.0).

When strong seasonal forces disturb this relatively stable system the pattern of seasonality interferes with the biological interaction (Fig. 2b). The prey-predator dynamics is strongly disturbed and the prey is not able to grow beyond its inoculum size ( $10 \text{ mg cl}^{-1}$ ) in the first season, consequently leading to a drastic decline in the predator population and a growth in the prey the second season that is controlled by seasonality (autumn) rather than by the predator. Decreasing  $K_{\text{prey}}$  to 200 (Fig. 2c) results in extinction of the prey species around time step 80, which would not be the result had seasonality not been imposed. This can be interpreted as an example of the increased vulnerability of a smaller prey population (and its predator) to the risks of a changing environment. Although these seasonal fluctuations are predictable, they interfere with the biological dynamics in a seemingly unpredictable manner (Tømte et al. 1998) and increase the probability of extinctions. Seasonality thus may severely interfere with biological dynamics in prey-predator systems. In Fig.

2d, the phase diagram representing the simulation from Fig. 2a, demonstrates the general feature of circular counterclockwise rotation in prey-predator systems.

We first simulate competition between equal competitors in a non-seasonal environment obtaining a stable equilibrium in which the two species coexist at around 60% of their carrying capacity (Fig. 3a).

By introducing seasonality and niche difference (Fig. 3b) to the same competitors, the stable equilibrium is displaced by oscillations largely produced by the seasonal forcing function. When living conditions are good (left side of the peaks of the curves) and as the joint biomasses increase to 50–60% of the  $K$  values (i.e. when resource scarcity occurs), the benefit of being the early starter increases as does the cost of being the late starter. However, by increasing  $K$  of the late starter by 25%, the effect of being an early starter is more than compensated (Fig. 3c). An increase of the  $K$  value of the late starter by only  $\sim 6\%$  is sufficient to give an even outcome of the competition. The phase portrait in (Fig. 3d) shows an unsymmetrical oval counterclockwise rotation when the early starter is depicted on the x-axis and the late starter is depicted on the y-axis.

When two mutualist species described by equal and standard parameters (Table 1) grow under non-seasonal conditions, they reach stable equilibrium populations at  $K$  (Fig. 4a). If we compare Fig. 3a (competition) and 4a (mutualism), we find that the mutualists grow to higher

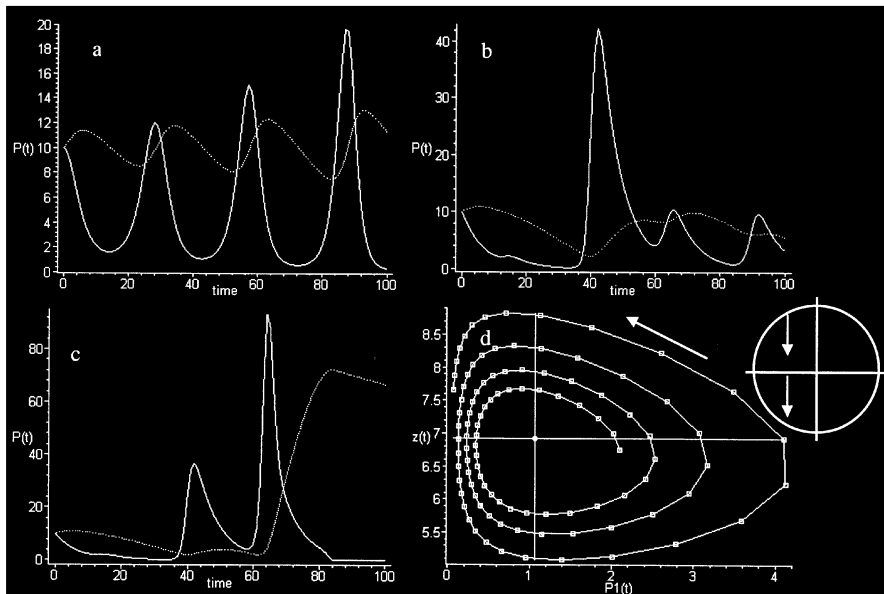


Fig. 2. Prey-predation. a) Lotka-Volterra cycles, no seasonal forcing (solid line, prey, dashed line, predator), b) seasonal forcing introduced, c) same as b, but decrease in prey carrying capacity ( $K_{\text{prey}} = 200$ ), d) normalized ( $1/\text{SD}$ ) phase portrait of the interaction in c, including characteristic directions from the PCA (see below).



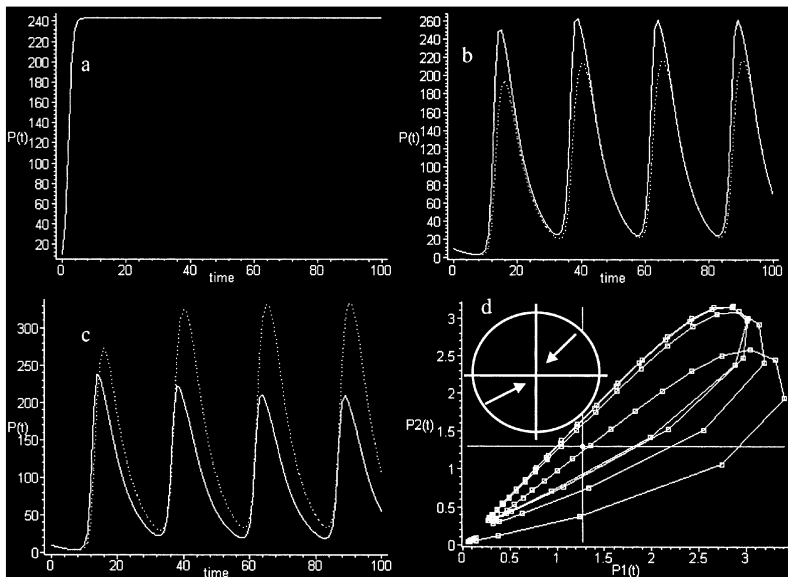


Fig. 3. Competition. a) Equilibrium between competitors having 100% niche overlap and without seasonal forcing, b) same competitors, but seasonality and temporal niche difference (14 days) is introduced (solid line P1 is early starter, see Table 1, standard P), c) 25% increase in K for the late starter reverse the outcome of the competition ( $K_1 = 400$ ,  $K_2 = 500$ ), d) normalized (1/SD) phase portrait of the competition in c, including characteristic directions from the PCA (see below).

biomass than the competitors. This difference ( $\sim 54\%$  increase in equilibrium biomass) is due to the mutualistic effects introduced by the parameters  $p$  and  $h$ . When seasonal forces are imposed on the mutualistic system, there is low interference with the biological dynamics (approximately 2% reduction in seasonal peak biomass) as compared to stable equilibrium in (Fig. 4a). Stable oscillations occur due to the seasonal force only, as seen from (Fig. 4b). If the late starter is given a 25% higher K, a mutualistic interaction imposes small changes on the interacting species as compared to competition (Fig. 2c) and both species reach their respective K values despite the seasonal forcing. It is interesting to note that changing from equal to different K values in a seasonal regime has much more pronounced effects in competitive than mutualistic interactions. If we compare Fig. 3c and 4c, we also see that when seasonality imposes the most severe growth conditions (i.e. the troughs on the curves), mutualists show similar performances in terms of biomass, whereas competitors produce more different biomasses.

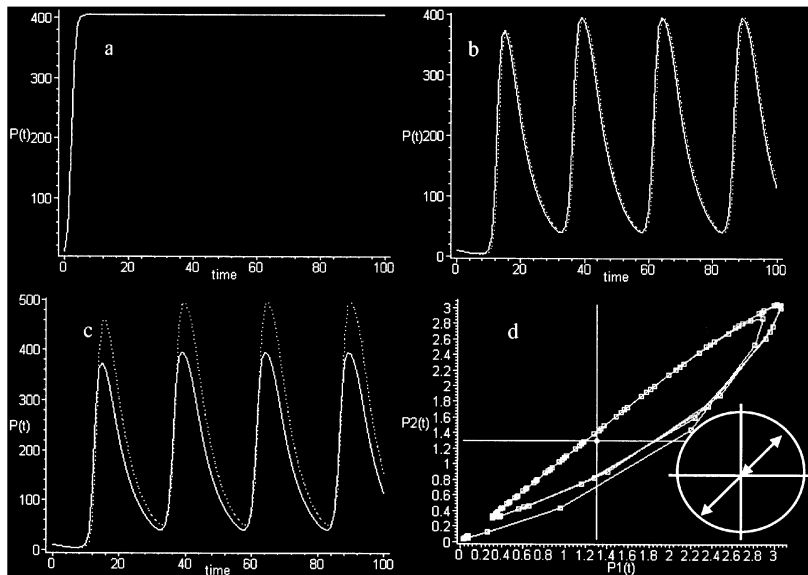
The phase portrait in Fig. 4d shows an oval counter-clockwise rotation around a  $45^\circ$  line with the x-axis (indication of mutualism) when the early starter is depicted on the x-axis and the late starter is depicted on the y-axis. The deviation from a straight line gives an indication of the strength of seasonal forces on mutualism as described by eq. 5 and 6.

Facilitation with standard parameters in a non-seasonal environment shows a stable equilibrium with the gainer species reaching (58%) higher populations than

the facilitator (Fig. 5a). As seasonality is introduced (Fig. 5b), the two species show somewhat different responses. The relative difference in seasonal maximal biomass increase to 63% in favour of the gainer and the corresponding difference in seasonal minimum biomass increases to 75%. The gainer population also fluctuates more strongly than the facilitator population in absolute terms. After seasonality has been imposed, the facilitator population fluctuates between  $\sim 9\%$  and  $\sim 91\%$  of the stable non-seasonal equilibrium population. The gainer population fluctuates between  $\sim 10\%$  and  $\sim 99\%$  of the stable non-seasonal equilibrium population. The facilitator-gainer trajectories also rotate counterclockwise when the facilitator is depicted on the x-axis and the gainer on the y-axis.

The higher fluctuations in the gainer population fit well with the assumption that the gainer having competitive characteristics, takes advantage of seasonality (i.e. grows relatively better in periods of resource scarcity when biomasses approaches K) and the facilitator, having mutualistic characters, "passively" rises or falls with the forces of seasonality. This can be explained by looking at the terms in eq. 7 and 8. The interspecific term ( $aG/K_F$ ) of eq. 7 describing the facilitator is a subtraction term and it grows with increasing G (i.e. the higher G, the more negative is the impact of the gainer on its facilitator). Likewise, the interspecific term ( $gF/(1+hF)$ ) of eq. 8 is an addition term that grows with increasing F. The net effect of these equations is amplified by seasonality. For instance, when seasonality (eq. 9) produces high growth rates for the two species around time step 10 (Fig. 5b), the gainer

Fig. 4. Mutualism. a) Equilibrium between facultative mutualists having 100% niche overlap without seasonal forcing, b) seasonal forcing and 14 days niche difference introduced, (solid line P1 is early starter), c) same as b, but 25% increase in K for the late starter, d) normalized (1/SD) phase portrait of the interaction in b, including characteristic directions from the PCA (see below).



population grows proportionately faster than the facilitator population because both populations are high and the interspecific effects of eq. 7 and 8 are strong. When seasonality again produces poor living conditions for both populations (i.e. around time step 30), both populations are low and the interspecific effects remain low.

Figure 5c and d illustrates the same situation when first the facilitator (c) is given 100% higher K than the

gainer and then (d) these parameter selections are reversed. The plates show that the facilitator cannot fully utilize a higher K value due to the competitive forces from the gainer, whereas the gainer population can reach its K.

The general pattern shown through these simulations is that seasonality seems to amplify interaction effects of a competitive nature (i.e. all negative interspecific

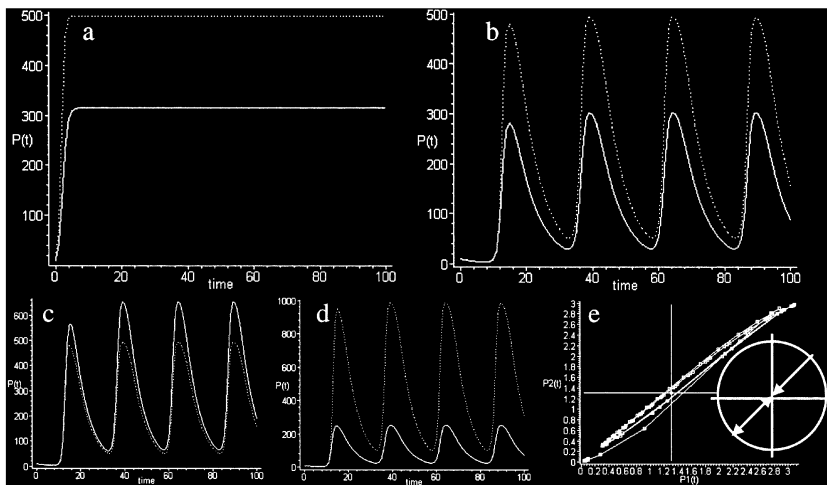


Fig. 5. Facilitation. a) Equilibrium between facilitator (solid line) and gainer, having 100% niche overlap without seasonal forcing, b) seasonal forcing introduced, c) same parameters as in b, but the facilitator have a 100% higher K than the gainer, d) same parameters as in b and c, but here the gainer have a 100% higher K than the facilitator e) normalized (1/SD) phase portrait of the interaction in b, including characteristic directions from the PCA (see below).

effects). When the gainer population has a higher  $K$  than its facilitator, the combined result of biological interaction and seasonality is dramatic and the gainer reaches a much higher population size than its benefactor, at all times except in the early growth phase (i.e. spring) when resources are ample.

To look at the effect of changing the frequency of seasonal forces, we also carry out a simple sensitivity analysis where we adjust the parameter  $\omega$  (which has a standard value of 0.25, thus creating four seasons within 100 time steps). This analysis is done with the prey-predation and competition models, as these interactions are the most affected by seasonal forcing. Our general finding is the same for the two interactions. At high frequencies ( $\omega > 0.25$ ), the distortions of the biological dynamics decrease with increasing values of  $\omega$ . On the other hand, when we simulate low frequency seasonal forcing with wavelengths of several years (i.e. large scale climatic fluctuations like the North Atlantic Oscillations or the El Niño), the relative impact of seasonal forces on the biological dynamics becomes increasingly stronger.

The broad result of these simulations is that predictable seasonal cycles interfere with all the four types of ecological interactions, but at a highly varying degree.

### Angle frequency method results and PCA

Without seasonality, our models produce all the standard phase portraits described in Materials and methods section. When seasonality is introduced, cyclic phase portraits emerge for all interactions. The basic direction of rotation in the phase portraits is conserved for the prey-predation interaction. In the case of mutualism the basic feature of a non-seasonal phase portrait is also kept as the trajectory circle around a  $v = 45^\circ$  line that extend through the origin. The competition phase portraits are quite different from those described in the methods section because we force the competitors to coexist by our selection of parameters.

Figure 6 is a PCA plot showing the results of an analysis of angle frequencies resulting from the 32 simulations where all interactions are subject to similar parameter manipulations (parameter settings 1–8 in Materials and methods section). Figure 6 show that within the span of parameter values used in this study, the angle frequencies (characteristic histograms) can identify all types of interaction. Prey-predation patterns are so different from all other interactions that the latter cluster in the PCA score plot (Fig. 6a). The loading plot (Fig. 6b) shows that quadrants 2 and 3 and the corresponding angles within the angle brackets  $[-94$  to  $-77]$ , and  $[-111$  to  $-94]$  identify prey-predation in the eight simulations. At this point in the analysis all we can say about the three other interac-

tions is that they are differentiated from prey-predation and characterized by angles within the angle brackets  $[-145$  to  $-128]$  in the first and third quadrants.

We repeated the PCA analysis, but this time without the prey-predator angle frequencies (Fig. 7). This is done because the main components of the total variance in the interactions are related to prey-predation, which then hide relevant differences among the other interactions.

Figure 7 shows that without the strong effect from the prey-predator angle frequencies, the AFM now differentiates among the other interactions. The score plot (Fig. 7a) shows that PC1 (the horizontal principal component axis) distinguishes facilitation from mutualism and competition. The vertical principal component axis (PC2) also distinguishes competition from mutualism (i.e. the competition-mutualism dimension). We see that manipulation of the parameters shift scores along the PC2 axis (competition-mutualism) dimension for mutualism and competition scores. The position of the facilitation point-swarm, between competition and mutualism along PC2, shows that the AFM detects that facilitation has both competitive and mutualistic properties. The loading plot (Fig. 7b) shows that internally the three interactions are distinguished by angles in the following angle brackets:  $[-145$  to  $-128]$  in quadrant 3 and  $[43$  to  $60]$  in quadrant 1 (mutualism),  $[-145$  to  $-128]$  in quadrant 2 and  $[-8$  to  $8]$  in quadrant 3 (competition) and  $[-162$  to  $-145]$  and  $[25$  to  $43]$  in quadrant 3 (facilitation). As an example, the angles that characterize mutualism are those that show how the species biomasses return to low/high values when they are already low or high respectively.

It should be noted that the PCA axes in Fig. 6 and 7 are not directly comparable, thus Fig. 6 can only indicate the difference between prey-predation and the group of the three other interactions and Fig. 7 can only indicate the corresponding difference between these three interactions. However, based on the PC1 and PC2 numerical scores, from the PCA score plot in Fig. 6, we can calculate an expression for the internal relationship between the different interactions as the absolute difference between average distances (centres of the point swarms) in the PC1 and PC2 directions (PC1 and PC2 units). In descending order we get the differences, 50.3 between prey-predation (P) and mutualism (M), 47.8 between P and facilitation (F), 46.5 between P and competition (C), 6.3 between M and F, 5.8 between C and M and 3.5 between C and F.

To measure the difference in sensitivity of parameter choices among the four interactions, we use the SVI and the variance within angle frequency classes (see Materials and methods and Table 2). The table shows that prey-predation is by far the most sensitive interaction (i.e. with the current choice of parameter values, it shows the most divergent response). Generally there is

good agreement between the two measures, but they give different results concerning which interaction is the least sensitive.

## Discussion

In the present study, we examine four types of reciprocal interaction and their responses to seasonal forcing by developing simulations, both in constant and seasonal environments. Our results show that conditions that would give stable equilibria, or limit cycles, in a constant environment (defined by the parameter sets in Table 1), for the four interactions, give rise to different time developments in a seasonal environment. To examine how differences in parameter values would influence the interactions in a seasonal environment, we change parameter values for a subset of the parameters (carrying capacity, intrinsic growth rate and response to abiotic factors) and make a set of 8 single simulations for each type of interaction. Based on the angle fre-

quency method AFM, the four interaction types can be distinguished from the “fingerprints” they leave in paired time trajectories. The principal component meta-analysis (Fig. 6) of the four interaction types shows that prey-predation is the type of ecological interaction that is most sensitive to changes in parameters, whereas facilitation and mutualism is least sensitive.

The simulations and their graphical interpretations indicate that the four different forms of ecological interaction are influenced by seasonality in two principally different ways. For competition and facilitator-gainer interactions, seasonality seems to amplify the effects of resource scarcity (density dependent interspecific effects). Seasonality reallocates the capacity of utilizing shared resources by redistributing advantages and disadvantages as compared to a constant environment. Chesson and Huntly (1997) also found such effects. A distinguishing feature of competition compared to the three other interaction types is the simultaneous increase of the two competitors when both competitors have low abundance combined with the

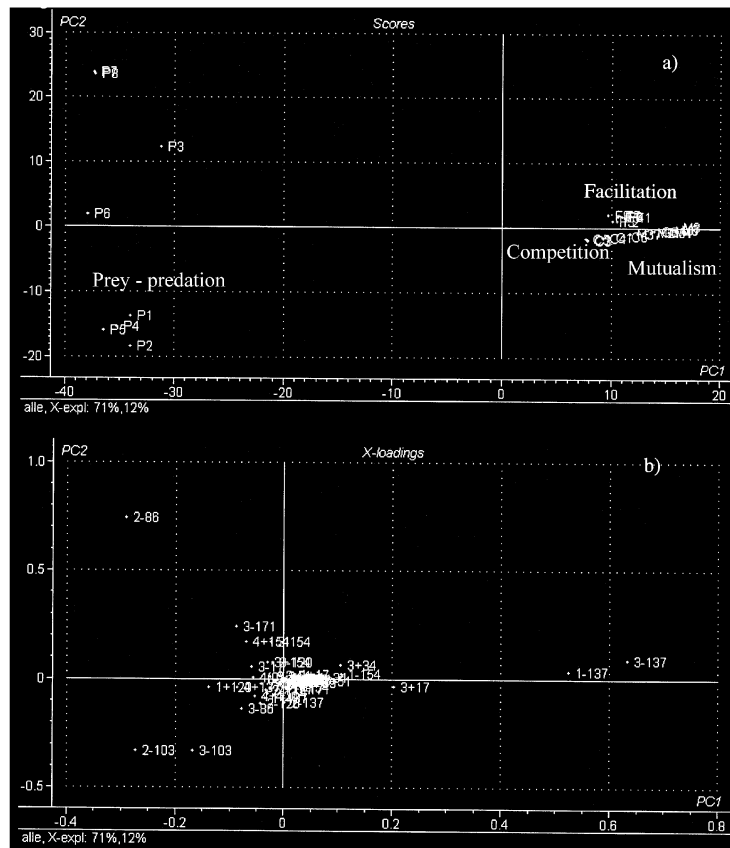


Fig. 6. PCA plots, x-axis is first principal component y-axis is second principal component. a) Score plot (upper) show the “position” of the different interactions. b) Loading plot (lower) identifies the characteristic directions of angles in the different phase portraits corresponding to the four types of interactions.



tems, seasonality appears to limit intrinsic cycles to one or two cycles, whereas intrinsic cycles in terrestrial systems (hare-lynx: Gilpin 1973; lemmings, voles: Turchin et al. 2000) may persist for longer times (decades). The large SVI and angle frequency variance for the prey-predator interaction (Table 2) suggests that this interaction type may be difficult to define in terms of a characteristic “fingerprint”. However, despite of the high sensitivity to parameter changes, prey-predation is isolated from the other interactions in the PCA (Fig. 6a) and thus easy to identify when compared to the three other interactions.

A distinguishing feature of prey-predation is the persistent circular counterclockwise rotation of trajectories when the prey is depicted on the x-axis and the predator on the y-axis. This feature follows from the rapid response of the predator to reduction in prey abundances and has been observed in several time series (McCauley and Murdoch 1987, Matveev 1995, Seip 1997). A distinguishing feature of mutualism is that both species decrease in concert.

A comparatively strong gainer will fluctuate markedly less than its benefactor, whereas a competitively weak gainer will fluctuate at nearly the same level as its benefactor.

Although it must be kept in mind that all simulations in this work relate to two-species interactions and therefore are not automatically relevant for multispecies contexts, the simulations demonstrate that the AFM has a potential for separating ecological interactions even if characteristics of the involved species change markedly. Studies of observed time series quoted above suggest that the “fingerprints” found for the theoretical time series also may be found in natural time series, and also in trajectories based on laboratory experiments.

*Acknowledgements* – We gratefully acknowledge three anonymous reviewers for critical and constructive comments.

## References

- Andersen, T. 1997. Pelagic nutrient cycles. Herbivores as sources and sinks. – Springer-Verlag.
- Bertness, M. D. and Callaway, R. 1994. Positive interactions in communities. – *TREE* 9: 191–193.
- Chesson, P. and Huntly, N. 1997. The roles of harsh and fluctuating conditions in the dynamics of ecological communities. – *Am. Nat.* 150: 519–553.
- Gilpin, M. 1973. Do hares eat lynx? – *Am. Nat.* 107: 727–730.
- Gurney, W. S. C. and Lawton, J. H. 1996. The population dynamics of ecosystem engineers. – *Oikos* 76: 273–283.
- Jones, C. G., Lawton, J. H. and Shachak, M. 1997. Positive and negative effects of organisms as physical ecosystem engineers. – *Ecology* 78: 1946–1957.
- Kjellberg, G. 1986–1998. Tiltaksorientert overvåkning av Mjøsa med tilloppselver. – Statlig program for forurensningsovervåkning, NIVA/SFT (in Norwegian).
- Kretzschmar, M., Nisbet, R. M. and McCauley, E. 1993. A predator-prey model for zooplankton grazing on competing algal populations. – *Theor. Popul. Biol.* 44: 32–66.
- Lindsley, E. G. 1958. The ecology of solitary bees. – *Hilgardia* 27: 543–599.
- Matveev, V. 1995. The dynamics and relative strength of bottom-up vs top-down impacts in a community of subtropical lake plankton. – *Oikos* 73: 104–108.
- Mazumder, A. and Havens, K. E. 1998. Nutrient-chlorophyll-Secchi relationships under contrasting grazer communities of temperate versus subtropical lakes. – *Can. J. Fish. Aquat. Sci.* 55: 1652–1662.
- McCauley, E. and Murdoch, W. W. 1987. Cyclic and stable populations: Plankton as a paradigm. – *Am. Nat.* 129: 97–121.
- McQueen, D. J., Post, J. R. and Mills, E. L. 1986. Trophic relationships in freshwater pelagic ecosystems. – *Can. J. Fish. Aquat. Sci.* 43: 1571–1581.
- Renshaw, E. 1991. Modelling biological populations in space and time. – Cambridge Univ. Press.
- Reynolds, C. S., Thomson, J. M., Ferguson, A. J. D. and Wiseman, S. W. 1982. Loss processes in the population dynamics of phytoplankton maintained in closed systems. – *J. Plankton Res.* 4: 561–600.
- Sarnelle, O. 1994. Inferring process from pattern: trophic level abundances and imbedded interactions. – *Ecology* 75: 1835–1841.
- Seip, K. L., Sas, H. and Vermij, S. 1991a. The ecosystem of a mesotrophic lake – I. Simulating plankton biomass and the timing of phytoplankton blooms. – *Aquat. Sci.* 53: 239–262.
- Seip, K. L., Sas, H. and Vermij, S. 1991b. The ecosystem of a mesotrophic lake – II. Interactions among nutrient load, river flow, and epilimnion depth. – *Aquat. Sci.* 53: 263–272.
- Seip, K. L. 1997. Defining and measuring species interactions in aquatic ecosystems. – *Can. J. Fish. Aquat. Sci.* 54: 1513–1519.
- Seip, K. L. and Reynolds, C. S. 1995. Phytoplankton functional attributes along trophical gradient and season. – *Limnol. Oceanogr.* 40: 589–597.
- Seip, K. L. and Pleym, H. 2000. Competition and predation in a seasonal world. – *Verh. Internat. Verein. Limnol.* 27: 823–827.
- Seip, K. L., Sas, H. and Vermij, S. 1992. Nutrient-chlorophyll trajectories across trophic gradients. – *Aquatic Sci.* 54: 58–76.
- Sommer, U., Gliwicz, Z. M., Lampert, W. and Duncan, A. 1986. The PEG-Model of seasonal succession of planktonic events in fresh waters. – *Arch. Hydrobiol.* 106: 433–471.
- Thompson, J. N. 1999. The evolution of species interactions. – *Science* 284: 2116–2118.
- Tømte, O., Seip, K. L. and Christoffersen, N. 1998. Evidence that loss in predictability (and possibly dynamic chaos) increase with increasing trophic level in aquatic ecosystems. – *Oikos* 82: 325–332.
- Turchin, P., Okanen, L., Ekerholm, P. et al. 2000. Are lemmings prey or predators? – *Nature* 405: 562–565.
- Wright, D. H. 1989. A simple, stable model of mutualism incorporating handling time. – *Am. Nat.* 134: 664–667.
- Yodzis, P. 1989. Introduction to theoretical ecology. – Harper & Row.